Radio-continuum survey of the Coma/A1367 supercluster. IV - 1.4 GHz observations of CGCG galaxies

Castillo, E. del; Gavazzi, G.; Jaffe, W.

THE ASTRONOMICAL JOURNAL VOLUME 95, NUMBER 5 MAY 1988

RADIO-CONTINUUM SURVEY OF THE COMA/A1367 SUPERCLUSTER. IV. 1.4 GHz OBSERVATIONS OF CGCG GALAXIES

E. DEL CASTILLO AND G. GAVAZZI
Istituto di Fisica Cosmica del CNR, Via Bassini 15, 20133 Milano, Italy

W. JAFFE
Sterrewacht Leiden, P.O. Box 9513, 2300 RA Leiden, The Netherlands
Received 30 October 1987; revised 21 January 1988

ABSTRACT

1.4 GHz radio-continuum observations of 148 CGCG galaxies in the Coma supercluster region were obtained with the VLA in C array configuration. Comparison with previous measurements at 0.6 GHz leads to an average spectral index $\langle\alpha\rangle = 0.8$. The structures of 29 galaxies in this region determined with high-resolution VLA (A array) observations are presented.

I. INTRODUCTION

This paper is focused on the radio-continuum emission from the galaxies in the Coma supercluster. This region was extensively surveyed with the Westerbork Synthesis Radio Telescope and with the Very Large Array.* The Coma cluster was observed by Jaffe, Perola, and Valentijn (1976, JPV); the cluster A1367 by Gavazzi (1979), four groups in the direction of the supercluster by Jaffe, Gavazzi, and Valentijn (1986, hereafter referred to as Paper I), and a sample of relatively isolated supercluster galaxies by Jaffe and Gavazzi (1986, Paper II). These data were analyzed and discussed in Gavazzi and Jaffe (1986, Paper III), where the average radio continuum properties of galaxies in this supercluster were derived as a function of galaxy morphology and local galaxy density. It was found that the radio emission from elliptical and S0 galaxies does weakly depend on the local galaxy density, while spiral galaxies in the two surveyed clusters develop radio sources 6–10 times brighter than spirals outside clusters. The analysis carried out at 1.4 GHz was based on 444 galaxies observed at 1.4 GHz and on 284 galaxies observed at 0.6 GHz and converted to 1.4 GHz using $\langle\alpha\rangle = 0.8$. To check the validity of this assumption, this paper presents new 1.4 GHz observations undertaken with the VLA in C array of 148 galaxies already surveyed at 0.6 GHz, for which we derive spectral-index information.

Another 29 galaxies already known to be radio sources have been observed at 1.4 GHz in A array in order to determine their radio morphologies. The C array observations are presented in Sec. II. In Sec. III we compare the present observations with the previous 0.6 GHz measurements. The A array observations are described in Sec. IV, and in Sec. V we briefly discuss the results obtained. $H_0 = 100$ km s^{-1} Mpc^{-1} is assumed throughout this paper.

II. C ARRAY: OBSERVATIONS AND DATA REDUCTION

One-hundred forty-eight CGCG (Zwicky and Herzog 1963) galaxies in the Coma supercluster region were observed on 27 September 1985 using the NRAO VLA (Thompson *et al.* 1980) in C array configuration of about 25 active antennas. The observing was done in two frequency bands centered at 1465 and 1515 MHz with a bandwidth of 50 MHz each. For the source 3C 286, which was used as primary calibrator, a flux of 14.4 Jy was assumed. Sources 1147 + 245, 1219 + 285, and 1323 + 321 were used as secondary calibrators. Four observations of 30 min each were obtained in the Coma cluster region. A 2 hr observation was centered on the southeast of A1367 near the radio galaxy 3C 264. Another eight fields of 10 min duration each were devoted to the galaxies in the four groups previously surveyed at 0.6 GHz (Paper I). We also report the analysis of a 90 min observation obtained on 29 May 1984 of the northwest periphery of A1367.

Table I gives the observation parameters of the fields surveyed in C array as follows:

Column 1: conventional field name.

Columns 2,3: (1950) right ascension and declination of the field center.

Column 4: duration in minutes of the observations.

Column 5: rms noise in the field (mJy/beam).

Column 6: CGCG galaxies included in the field of view.

Column 7: FWHM of the beam (arcsec).

Large maps (1024×1024 points) were synthesized and cleaned using the MX routine in the NRAO AIPS package. The details of the reduction procedure are identical to those described in Paper II. The rms noise varied from 0.1 mJy/beam to 0.5 mJy/beam except in A1367SE (1 mJy/beam) due to confusion from the strong source 3C 264 ($\approx$5 Jy).

Table II lists the 37 galaxies detected at 1.4 GHz in C array. The information is arranged as follows:

Columns 1,2,3: CGCG, UGC (Nilson 1973), and NGC names.

Columns 4,5: 1950 optical coordinates of the galaxy, with an accuracy of a few seconds of arc.

Column 6: apparent photographic magnitude according to CGCG.

Column 7: morphological type (0 = E, 1 = S0, 2 = S0a, 3 = Sa, 4 = Sab, 5 = Sb, 6 = Sbc, 7 = Sc, 8 = Scd–Irr, 9 = S...) taken from the literature, or estimated on the glass copy of the Palomar Sky Survey.

Columns 8,9: major and minor optical diameters in arcminutes (only for spiral galaxies). These were taken from the UGC catalog or measured on the blue plates of the Palomar Sky Survey.

Columns 10,11: galaxy recessional velocity with reference.

Column 12: adopted distance in megaparsecs derived assuming $H_0 = 100$ km s^{-1} Mpc^{-1}. This was computed from the mean recessional velocity of the group or cluster to which the galaxy belongs or, for isolated galaxies, from their own redshift (see col. 13).

*The National Radio Astronomy Observatory is operated by Associated Universities, Inc., under contract with the National Science Foundation.

TABLE I. Observation parameters of the fields surveyed in C array.

(1) field	(2) R.A. (h m s)	(3) Dec. (° ′ ″)	(4) dur. (min)	(5) rms (mJy/beam)	(6) surveyed galaxies	(7) FWHM (″)
A1367NW	114038.0	201657.0	90	0.09	97063 97064 97062 97068 97072 97073 97074 97079 97086 97087 97089 97090 97091 97092 97095 97096 97097 97100 97106	15.0X14.0
A1367SE	114200.0	200000.0	120	1.00	97088 97094 97093 97099 97101 97105 97109 97110 97113 97114 97115 97117 97118 97119 97120 97124 97125 97127 97128 97131	16.3X16.2
Coma1	125542.0	284500.0	30	0.25	160043 160044 160049 160055 160058 160057 160061 160214	16.8X15.8
Coma2	125530.0	273700.0	30	0.36	160064 160067 160074	15.4X15.3
Coma3	125500.0	274700.0	30	0.31	160020 160026 160037 160039 166040 160042 160046 160068 160070	15.5X15.3
Coma4	125918.0	281200.0	30	0.15	160086 160251 160253 160254 160255 160256 160257 160258 160259 160260 160261 160092 160093 160094 160095 160097 160100 160101 160103 160105 160104 160106 160108 160110 160112 160113 160115 160116	15.6X15.3
Group1	120140.0	203130.0	10	0.28	98034 98039 98040 128006 128008 98041 128009 98042 98045 128013 98046 128019 128018	16.7X14.9
Group2	120318.0	204759.0	10	0.29	128020 128022 128023 128024 128025 128026	16.5X14.8
Group3	114730.0	212525.0	10	0.21	127062 127063 127067 127069 127068 127071 127074	17.2X17.2
Group4	115010.0	210500.0	10	0.20	127082 127083 127085 127088 127089 127092 127095 127096	15.6X15.5
Group5	115530.0	252430.0	10	0.55	127110 127111 127112 127114 127117 127118 127120 127121 127123 127122	15.4X15.4
Group6	131420.0	311500.0	10	0.36	160173 160175 160176 160180 160181	15.7X15.1
Group7	131606.0	314418.0	10	0.26	160183 160185 160187 160193	15.7X15.1
Group8	131727.0	310516.0	10	0.25	160186 160190 160191 160195 160199 160200 160201 160203	15.7X15.3

Column 13: aggregation parameter (see Gavazzi (1987) for details): (1,2,3 = clusters; 5 = supercluster groups; 6 = supercluster pairs; 7 = supercluster isolated galaxies; 8–18 = foreground groups; 19 = background galaxies).

Column 14: absolute photographic magnitude corrected for internal absorption according to Haynes and Giovanelli (1984).

Columns 15,16: differences between optical and radio positions (optical − radio) in arcseconds.

Column 17: identification class: ID = 1,2, good; ID = 3, dubious (see Paper I).

Column 18: primary-beam attenuation factor (see Paper II).

Column 19: sky flux in millijanskys derived from the total map flux divided by the attenuation factor. For pointlike or slightly extended sources, the integrated flux density was derived by fitting a two-dimensional Gaussian to the emission. For extended sources, the total flux was obtained by numerical flux integration corrected for beam-to-pixel ratio.

Column 20: logarithm of the radio luminosity in W/Hz at the adopted distance.

Column 21: spectral index α defined as $S(\nu) = K\nu^{-\alpha}$.

Column 22: largest angular size of the radio source in arcseconds. For slightly extended sources, it corresponds to the major axis of the Gaussian fitted to the data. For extended sources, it is derived from contour maps.

Figure 1 shows the contour maps of the interesting sources observed in C array. Finding charts of the newly detected galaxies in A1367 (97089, 97092, 97114, and 97120) and in the Coma cluster (160046, 160106, and 160108) are given in Fig. 2 [Plate 75]. The finding charts of the remaining newly detected galaxies (in the supercluster groups) can be found in Paper I.

The 111 undetected galaxies are listed in Table III, arranged similarly to Table II except that the 4σ upper limit to the 1.4 GHz luminosity is given.

TABLE II. Galaxies detected in C array.

(1)	(2)	(3)	(4)	(5)	(6)	(7)	(8)	(9)	(10)	(11)	(12)	(13)	(14)	(15)	(16)	(17)	(18)	(19)	(20)	(21)	(22)
CGCG	UGC	NGC	R.A.	Dec.	m_p	T	a	b	Vel	R	Dist	A	M_p	$\alpha_0-\alpha_r$	S_0-S_r	ID	att	S_{sky}	log P	α	LAS
			(h m s)	(° ′ ″)			(′)	(′)	(Km/s)		(Mpc)			(″)	(″)			(mJy)	(W/Hz)		(″)
97068	-	-	113948.75	202346.6	14.7	6	1.1	0.7	5976	2	65.0	3	-19.58	0.88	-0.50	1	0.58	8.14	21.61	1.41	-
97073	-	-	114020.75	201441.8	15.6	8	0.5	0.5	7275	24	65.0	3	-18.46	-0.82	-1.50	2	0.96	17.04	21.94	0.63	58
97079	-	-	114037.50	201656.8	15.7	8	0.5	0.4	7000	24	65.0	3	-18.47	0.00	-0.75	2	1.01	3.87	21.29	2.38	25
97087	6697	-	114113.19	201449.1	14.3	8	1.7	0.3	6723	24	65.0	3	-20.56	2.64	0.00	2	0.82	58.06	22.47	0.89	120
97089	6701	3837	114120.75	201018.1	14.2	0	-	-	6248	10	65.0	3	-19.86	3.52	-5.31	1	0.65	1.53	20.89	<1.60	-
97092	-	-	114122.56	202745.7	15.5	2	0.5	0.3	6373	24	65.0	3	-18.65	3.51	3.50	1	0.50	2.88	21.16	<2.43	-
97091	6702	3840	114123.44	202116.1	14.7	6	1.1	0.7	7369	2	65.0	3	-19.58	2.64	0.31	1	0.67	2.29	21.06	1.78	-
97095	6704	3842	114126.62	201335.4	13.3	0	-	-	6180	16	65.0	3	-20.76	1.64	0.13	1	0.65	15.54	21.90	1.16	-
97114	-	-	114211.70	20 3 2.0	15.4	8	0.4	0.3	8293	25	65.0	3	-18.80	-7.63	-0.25	1	0.97	4.03	21.31	<2.25	-
97120	6718	3860	114213.50	20 416.0	14.5	3	1.2	0.6	6354	10	65.0	3	-19.74	-2.05	-4.75	1	0.94	4.69	21.37	<2.09	-
97127	6723	3862	114229.62	1953 2.2	14.0	0	-	-	6462	10	65.0	3	-20.06	0.00	-0.19	2	0.76	5333.04	24.43	0.79	540
127088	6851	3937	1150 7.81	205434.2	14.0	0	-	-	6618	10	70.0	5	-20.23	-1.93	-3.50	1	0.73	2.65	21.19	0.97	-
127092	-	-	115036.31	205612.1	15.3	0	-	-	--	-	70.0	5	-18.93	0.00	-1.00	1	0.71	52.39	22.49	0.30	-
127110	6928	3987	115446.69	252825.1	14.4	5	2.3	0.4	4495	24	46.5	11	-19.86	-0.68	1.31	2	0.72	33.69	21.94	0.63	78
127123	6966	4018	1156 6.50	253545.5	14.7	4	1.8	0.3	4479	24	46.5	11	-19.42	3.16	8.44	1	0.55	5.06	21.12	2.21	-
98040	7044	4061	12 127.87	203038.0	14.4	0	-	-	7336	10	70.0	5	-19.83	-1.87	-0.56	2	0.99	316.81	23.27	0.03	150
98042	7050	4065	12 132.81	203047.7	14.0	0	-	-	6374	10	70.0	5	-20.23	1.58	-0.19	1	1.00	3.40	21.30	<3.54	-
98041	7049	-	12 136.12	202746.8	15.7	8	1.0	0.1	7551	25	70.0	5	-19.59	-5.39	-0.25	2	0.97	2.46	21.16	<3.90	30
128013	-	4074	12 156.25	203540.6	15.4	1	-	-	6600	8	70.0	5	-18.91	2.46	0.56	1	0.93	2.02	21.07	1.34	-
98046	7061	4076	12 159.31	202859.2	14.3	9	0.9	0.9	6220	24	70.0	5	-19.93	4.33	-10.88	1	0.94	2.12	21.09	1.55	-
128023	7087	4092	12 317.00	204518.7	14.4	3	1.1	1.1	6719	2	70.0	5	-19.83	-1.05	0.44	1	0.99	9.38	21.74	<2.65	-
128024	-	4093	12 318.31	204759.0	15.3	0	-	-	--	-	70.0	5	-18.93	1.29	-2.06	1	1.01	80.65	22.67	0.25	-
128025	-	4095	12 321.00	2051 2.8	14.6	0	-	-	7057	9	70.0	5	-19.63	1.34	0.00	1	0.99	3.35	21.29	0.76	-
128026	7091	4098	12 330.56	2053 5.7	14.5	0	-	-	7330	10	70.0	5	-19.73	1.93	15.13	3	0.92	2.17	21.10	1.40	-
160039	8070	4839	125459.00	2746 6.6	13.6	0	-	-	7446	10	69.0	2	-20.59	-1.27	3.81	2	1.01	74.54	22.63	1.00	34
160046	-	4842	125510.65	274546.9	14.9	0	-	-	7496	12	69.0	2	-19.29	1.33	-0.31	1	0.99	1.87	21.03	<1.33	-
160055	8082	4848	125540.69	283044.4	14.2	8	1.5	0.3	7049	1	69.0	1	-20.74	-0.22	-0.63	1	0.54	23.21	22.12	0.73	-
160058	-	-	125544.81	285841.0	15.5	6	1.0	0.3	7609	1	69.0	2	-19.28	-1.15	6.75	1	0.57	1.54	20.94	2.35	-
160064	-	-	125610.19	2732 2.6	15.4	8	0.4	0.4	7368	24	69.0	2	-18.79	5.04	-3.94	1	0.74	1.95	21.05	1.65	-
160260	8128	4911	125831.00	28 336.0	13.7	5	1.0	0.7	7970	1	69.0	1	-20.68	-6.01	-1.06	1	0.58	18.12	22.01	0.72	-
160095	8134	4921	1259 1.50	28 917.3	13.7	5	2.5	2.0	5470	2	69.0	1	-20.61	-0.83	1.00	2	0.96	6.47	21.57	0.15	50
160105	-	4927	125933.19	281627.4	14.8	1	-	-	7572	12	69.0	1	-19.39	0.94	-0.63	2	0.93	7.08	21.61	0.34	20
160106	-	-	125943.00	2755 6.0	15.1	8	0.6	0.4	7175	1	69.0	2	-19.28	-2.87	-2.50	1	0.38	1.56	20.95	<2.00	-
160108	-	-	125948.50	282859.9	15.5	8	0.4	0.4	8323	12	69.0	2	-18.69	-4.28	0.38	2	0.36	7.65	21.64	<0.25	45
160173	8337	5056	131351.56	311248.5	13.6	7	1.9	0.9	5596	2	56.0	16	-20.52	-2.46	-2.19	1	0.90	3.99	21.17	1.50	-
160187	-	-	131620.19	314819.6	15.6	1	-	-	--	-	70.0	5	-18.82	1.91	1.19	1	0.95	8.03	21.67	0.78	-
160200	-	-	131754.87	31 942.4	15.5	1	-	-	--	-	70.0	5	-18.81	3.74	1.38	1	0.87	2.28	21.13	1.51	-

III. COMPARISON WITH THE 0.6 GHz OBSERVATIONS

Virtually all galaxies previously detected at 0.6 GHz (Gavazzi 1979; JPV and Paper I) were also detected in the present survey, with some exceptions which are listed in Table IV along with their limiting 1.4 GHz flux. In particular, the identification of 160183 (ID = 1 in Paper I) has been rejected due to improved radio position consequent to the higher resolution of the present observations. On the other hand, 128023, which was classified as a dubious identification in Paper I, has been resolved in two components, the fainter of which is associated with the galaxy (see contour map).

Ten other galaxies, which were undetected at 0.6 GHz, have been detected in the present survey. Among these, 97114 and 97120 were confused at 0.6 GHz by the radio galaxy 3C 264, and 98041 and 98042 were confused by 98040. The last four galaxies listed in Table IV, which were detected at 0.6 GHz with a dubious identification (ID = 3), have now a better radio/optical coincidence (ID = 1). We point out a misprint in Paper I: galaxy 127110, whose published sky flux at 0.6 GHz is $S = 15.16$ mJy, should be corrected in $S = 58.9$ mJy. At 1.4 GHz, we derive for this source a total flux of 33.7 mJy (Table II), not consistent with the value given in Burns *et al.* (1987) (54.8 mJy). The reason for missing flux in our observation is not well understood.

For the wide-angle-tail radio galaxy associated with galaxy 98040 (see Fig. 1(c)), we derive an integrated 1.4 GHz flux density consistent with that found by Burns *et al.* (1987). This, combined with the 0.6 GHz flux density, leads to an uncomfortably flat spectral index $\alpha = 0.03$ for such an extended source. However, the estimate of the 0.6 GHz flux was obtained by fitting three Gaussian components to the data. This method resulted in an underestimate of the extended flux. Numerical integration of the flux density of this source leads to $S_{0.6} = 498$ mJy and consequently to $\alpha = 0.52$ (Table VI).

We point out that sources 159072 and 127025 observed in C array (Paper II) have flux-density determinations consistent with those published in Hummel *et al.* (1987). The integrated flux density of 160039 (this paper) is consistent with that given in Parma *et al.* (1986).

The radio galaxy 3C 264 (97127, Fig. 1(a)) was mapped at lower resolution with the WSRT (Gavazzi, Perola, and Jaffe 1981), yielding results consistent with those obtained in this work. In particular, the flux densities derived in the two observations are consistent within 2%.

IV. THE A ARRAY OBSERVATIONS

Twenty-nine galaxies listed in Table V were observed on 9 and 10 March 1986 with the VLA in A array. These were

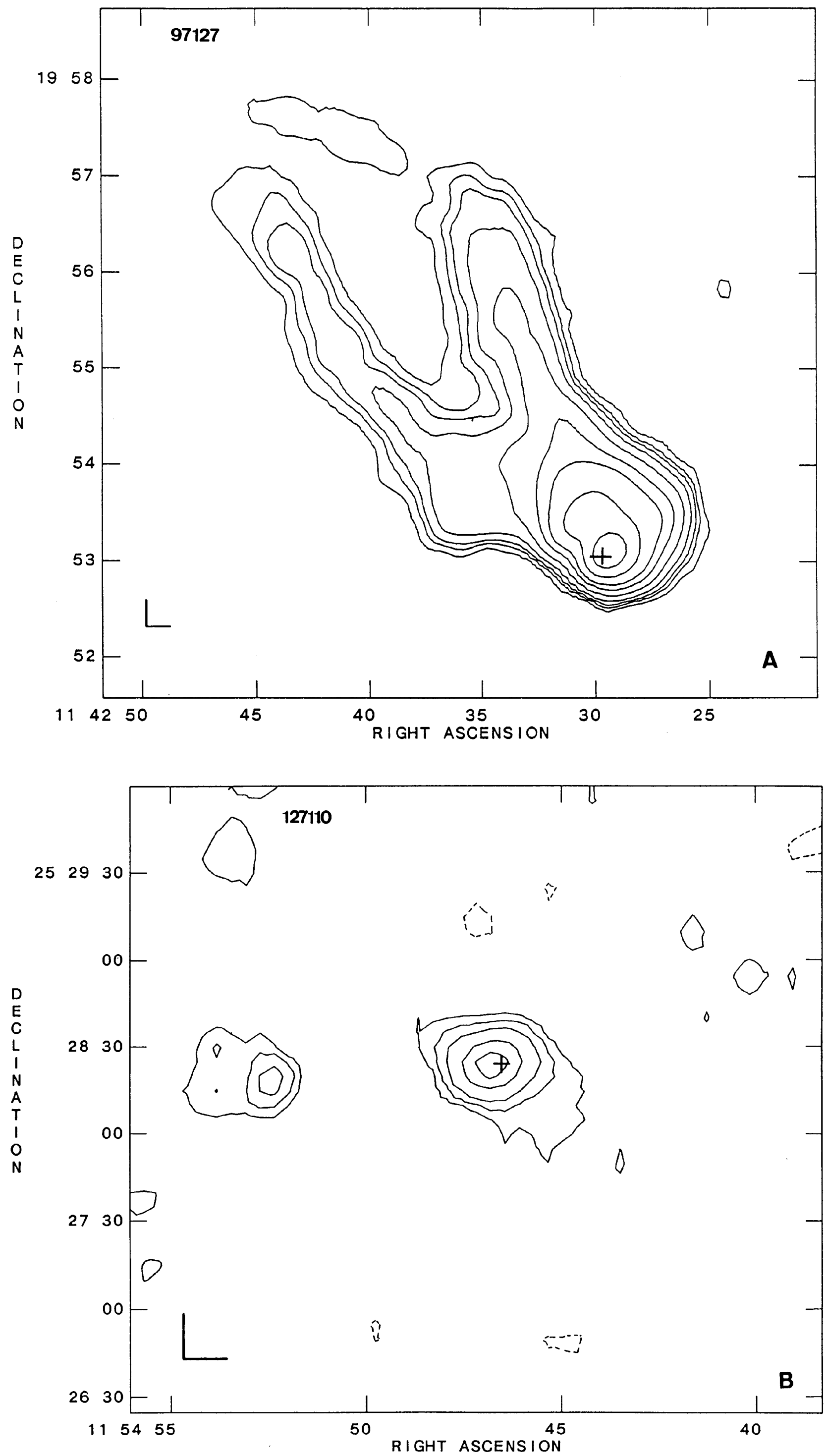

FIG. 1. Contour maps of the interesting galaxies detected in C array (uncorrected for primary-beam attenuation). The cross marks the position of the galaxy. The L shaped symbol in the lower left-hand corner indicates the FWHM of the beam. (a): 97127 = 3C 264 (levels: 2.4, 4.8, 7.2, 12.0, 24.0, 48.0, 80.0, 160.0, and 320.0 mJy/beam). (b): 127110 (levels: 1.23, 2.1, 3.5, 7.0, and 10.5 mJy/beam). (c): 98040, 98041, 98042 (levels: 0.7, 1.2, 2.0, 4.0, 6.0, and 10.0 mJy/beam). The inset shows the A array map of the inner part of 98040 (levels: 0.48, 0.96, 1.44, and 2.88 mJy/beam). (d): 128023 (levels: 0.7, 1.2, 2.0, 4.0, 6.0, 10.0, 20.0, 40.0, and 80.0 mJy/beam). (e): 160039 (levels: 1.1, 2.2, 3.2, 5.4, and 10.8 mJy/beam). The inset shows the A array map (levels: 0.4, 0.7, 1.2, and 2.4 mJy/beam). (f): 160095 (levels: 0.3, 0.45, 0.6, and 0.9 mJy/beam). (g): 160105 (levels: 0.4, 0.8, 1.2, 2.0, 3.9, 7.8, and 13.0 mJy/beam). (h): 160173 (levels: 0.9, 1.5, 2.5, and 5.0 mJy/beam).

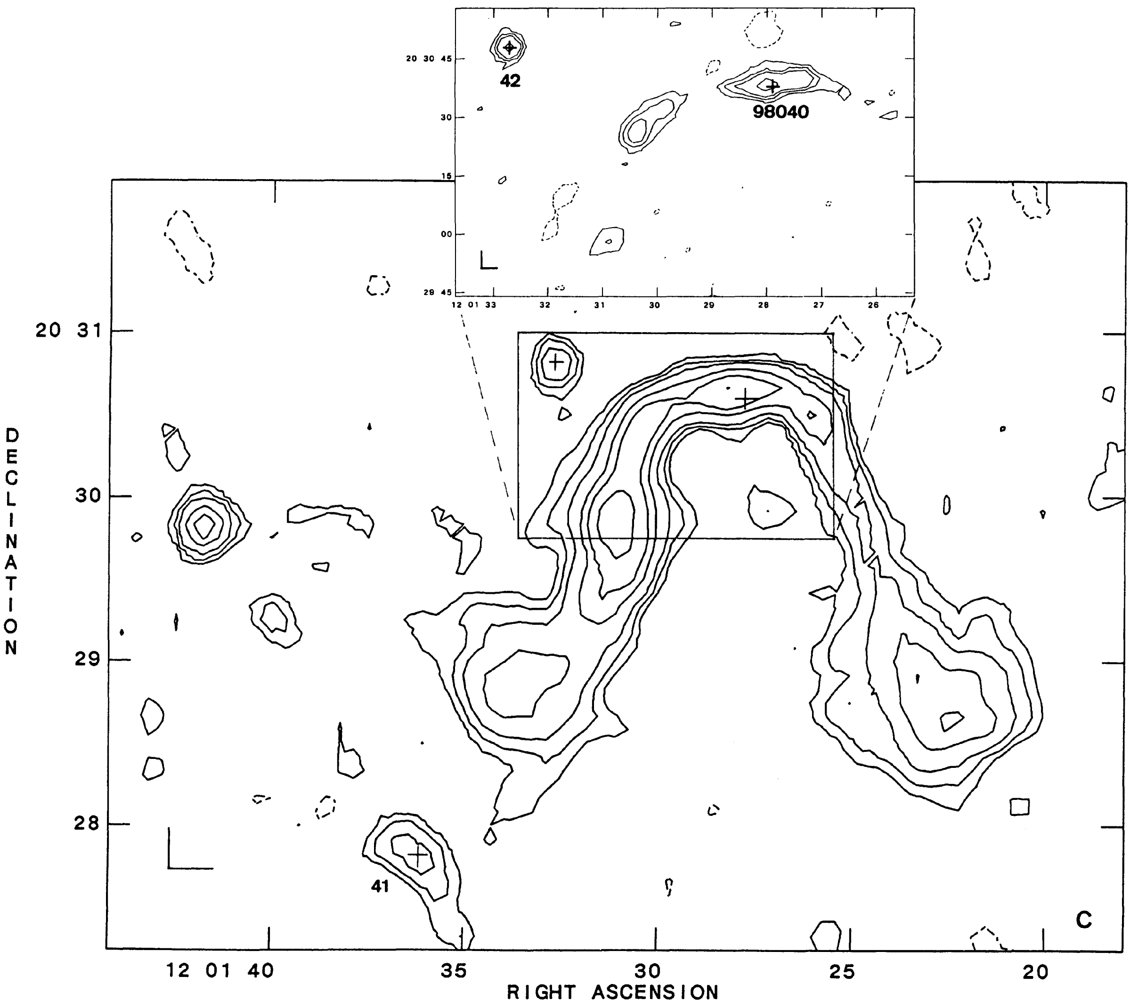

FIG. 1. (continued)

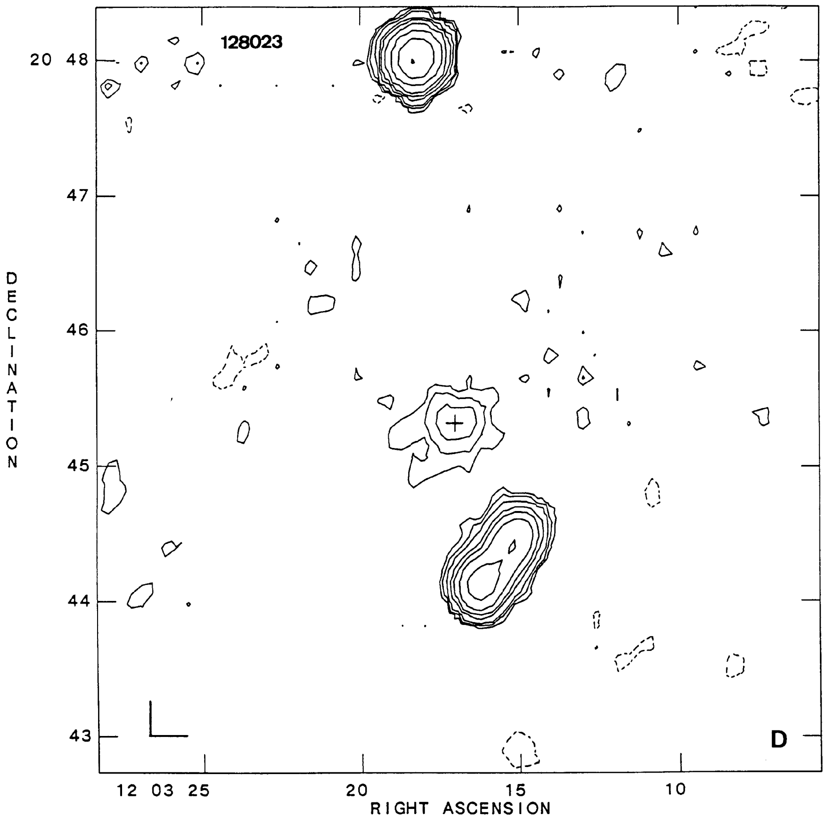

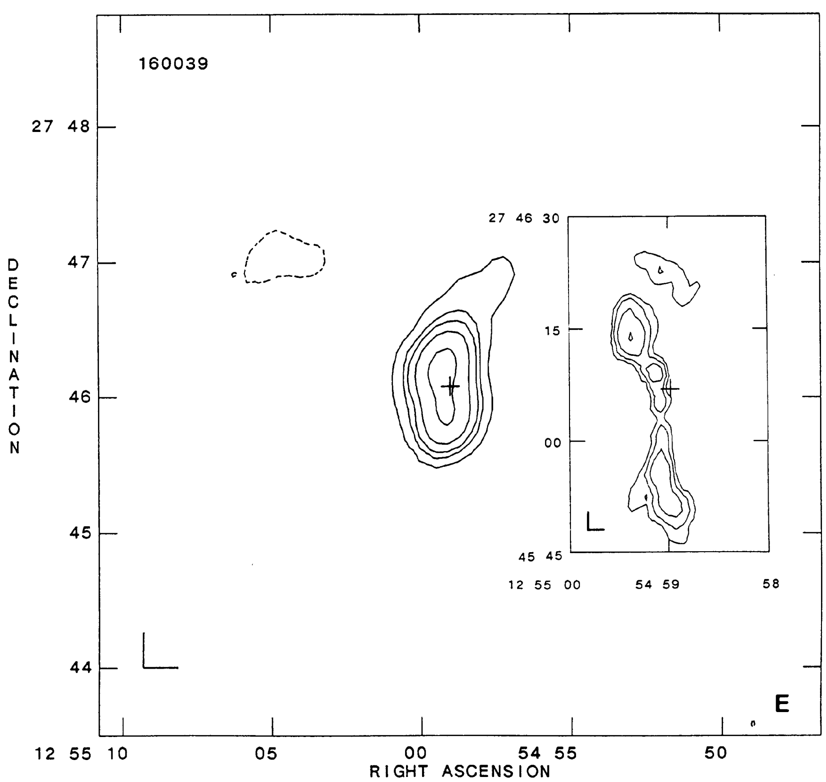

FIG. 1. (continued)

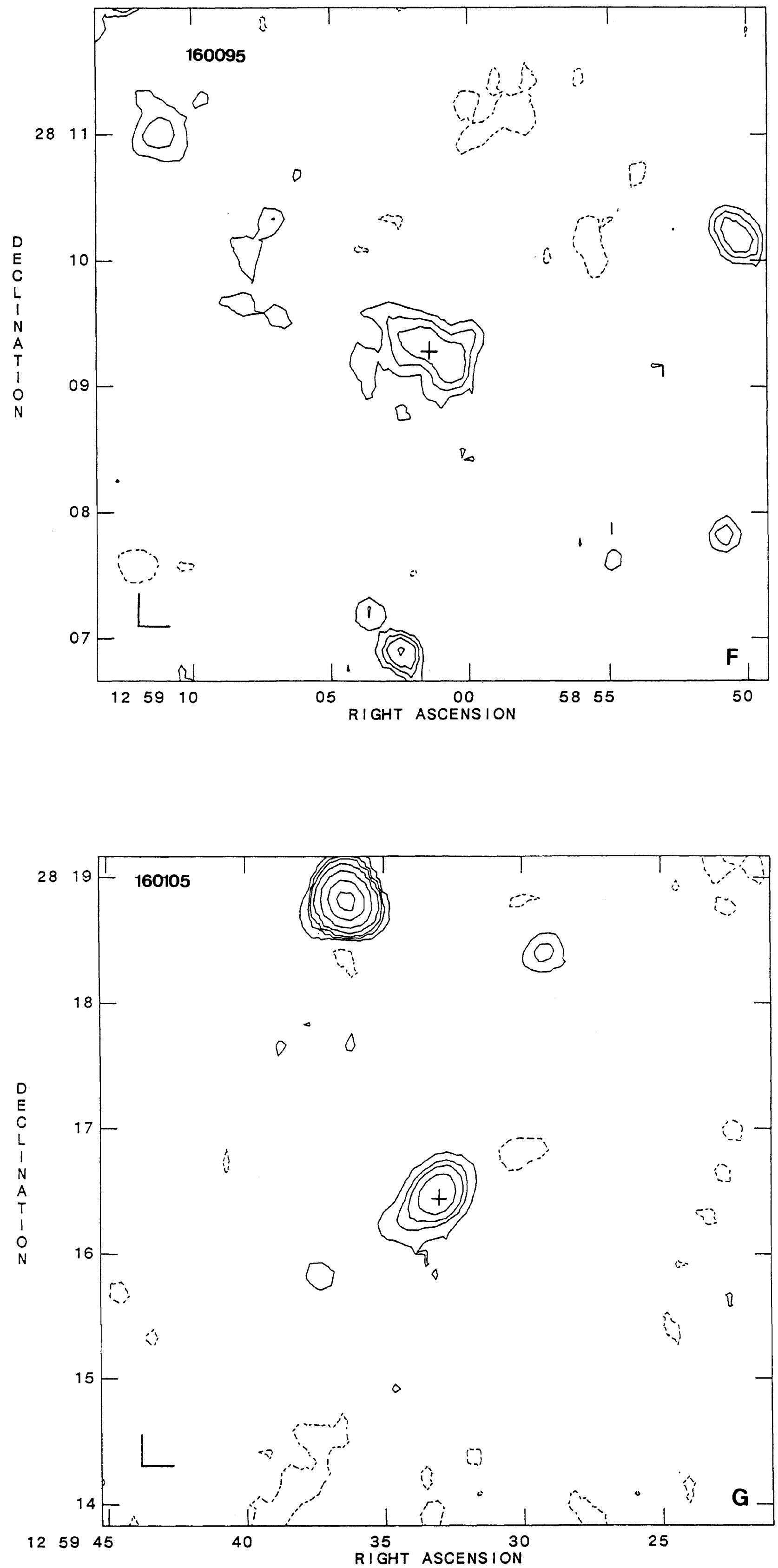

FIG. 1. (continued)

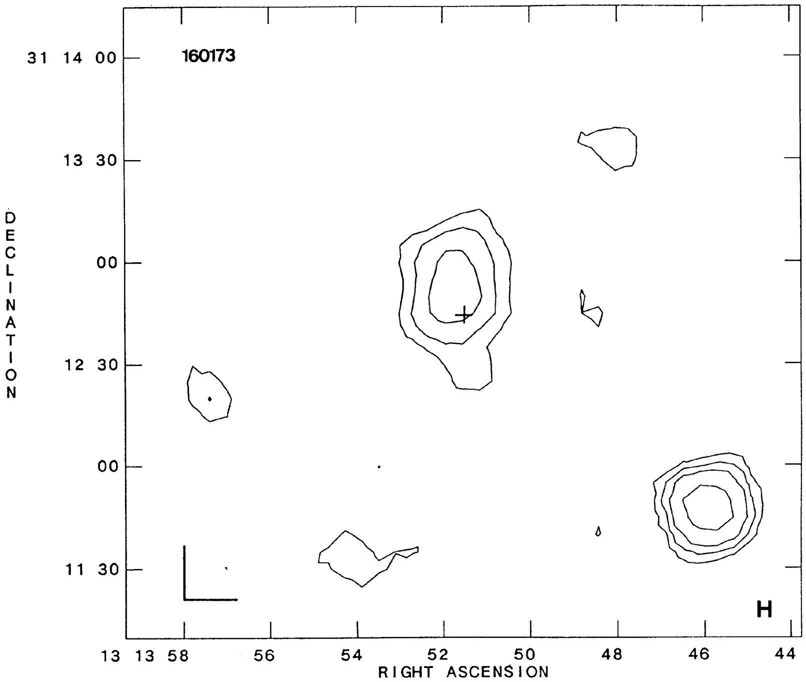

FIG. 1. (continued)

TABLE III. Galaxies undetected in C array.

(1)	(2)	(3)	(4)	(5)	(6)	(7)	(8)	(9)	(10)	(11)	(12)	(13)	(14)	(15)	(16)
CGCG	UGC	NGC	R.A.	Dec.	m_p	T	a	b	Vel	R	Dist	A	M_p	Att	log P
97063	-	-	113936.00	2019 0.0	15.7	9	0.4	0.2	6102	25	65.0	3	-18.48	0.55	<20.52
97064	-	-	113938.19	202233.0	15.6	9	0.5	0.2	5968	25	65.0	3	-18.62	0.50	<20.56
97062	-	-	113939.00	201518.0	15.5	8	0.8	0.3	7800	1	65.0	3	-19.02	0.55	<20.52
97072	-	-	114011.00	201818.0	15.0	3	0.9	0.5	6334	1	65.0	3	-19.22	0.90	<20.30
97074	-	-	114018.00	2021 0.0	15.4	0	-	-	--	-	65.0	3	-18.66	0.91	<20.30
97086	-	-	114111.04	2019 1.2	15.7	1	-	-	6328	8	65.0	3	-18.52	0.84	<20.34
97088	-	-	114123.90	20 324.7	15.2	1	-	-	5552	8	65.0	3	-18.95	0.79	<21.41
97090	-	-	114122.00	201353.5	15.3	1	-	-	5969	12	65.0	3	-18.76	0.71	<20.41
97094	-	-	114127.52	20 445.6	15.7	0	-	-	7950	17	65.0	3	-18.36	0.80	<21.40
97096	-	3841	114126.63	201459.3	15.0	0	-	-	6350	17	65.0	3	-19.06	0.67	<20.43
97097	6705	3844	114124.00	2018 0.0	14.9	2	1.4	0.2	6824	18	65.0	3	-19.50	0.71	<20.41
97093	-	-	114126.31	20 336.0	15.5	5	1.1	0.4	4857	11	65.0	3	-19.10	0.81	<21.40
97099	-	-	114132.01	20 056.6	15.7	0	-	-	7661	8	65.0	3	-18.36	0.90	<21.35
97100	-	3845	114129.91	201627.7	15.1	1	-	-	5643	16	65.0	3	-19.03	0.64	<20.45
97101	-	-	114143.51	20 723.2	15.3	2	0.4	0.3	6381	8	65.0	3	-18.81	0.83	<21.39
97105	-	-	114143.69	20 723.0	15.4	2	0.4	0.3	5439	18	65.0	3	-18.71	0.83	<21.39
97106	-	3851	114144.71	201531.3	15.2	1	-	-	6398	8	65.0	3	-18.98	0.47	<20.59
97109	-	-	114152.71	20 047.6	15.5	0	-	-	6751	8	65.0	3	-18.56	1.00	<21.31
97110	-	-	114149.47	20 622.0	15.5	1	-	-	4456	8	65.0	3	-18.68	0.89	<21.36
97113	-	-	114210.19	20 2 3.0	15.6	0	-	-	6350	17	65.0	3	-18.46	0.99	<21.31
97115	-	-	114211.85	20 916.4	15.5	1	-	-	7792	8	65.0	3	-18.72	0.76	<21.42
97117	-	3857	114214.56	194838.1	15.1	1	-	-	6183	3	65.0	3	-19.03	0.65	<21.49
97118	-	-	114216.58	195326.2	15.7	0	-	-	6484	8	65.0	3	-18.36	0.86	<21.37
97119	-	-	114212.81	195755.0	15.7	3	0.5	0.4	5256	11	65.0	3	-18.42	0.98	<21.32
97124	-	-	114222.00	20 011.0	15.3	0	-	-	--	-	65.0	3	-18.76	0.94	<21.33
97125	-	-	114218.69	20 312.0	15.6	7	0.8	0.5	8288	25	65.0	3	-18.70	0.94	<21.33
97128	-	-	114228.33	195355.9	15.2	0	-	-	6273	8	65.0	3	-18.86	0.80	<22.80
97131	-	-	114239.39	20 724.6	15.1	0	-	-	7646	18	65.0	3	-18.96	0.66	<21.49
127062	-	-	114655.19	211915.4	15.5	1	-	-	--	-	70.0	5	-18.85	0.74	<20.82
127063	6800	3910	114724.19	213641.4	14.4	0	-	-	7840	10	70.0	5	-19.83	0.68	<20.86
127067	-	-	1148 4.44	2111 7.1	15.5	1	-	-	--	-	70.0	5	-18.78	0.44	<21.05
127069	-	-	114816.00	2140 1.9	15.7	1	-	-	--	-	70.0	5	-18.70	0.37	<21.13
127068	-	-	114817.62	212651.2	15.3	8	0.6	0.4	--	-	70.0	5	-19.11	0.69	<20.85

TABLE III. (continued)

(1) CGCG	(2) UGC	(3) NGC	(4) R.A.	(5) Dec.	(6) m_p	(7) T	(8) a	(9) b	(10) Vel	(11) R	(12) Dist	(13) A	(14) M_p	(15) Att	(16) log P
127071	-	-	114820.62	212524.2	15.4	8	0.5	0.3	6388	24	70.0	5	-19.06	0.66	<20.87
127074	-	-	114839.75	211647.0	15.0	1	-	-	--	-	70.0	5	-19.31	0.36	<21.14
127082	-	-	114924.81	212314.3	14.7	7	0.9	0.7	6654	2	70.0	5	-19.65	0.24	<21.28
127083	-	-	114945.06	212248.4	15.1	8	0.6	0.5	6743	6	70.0	5	-19.21	0.34	<21.14
127085	-	-	114955.81	205413.5	15.5	9	0.9	0.3	--	-	70.0	5	-18.92	0.68	<20.84
127089	6852	3940	115011.62	2116 2.6	14.3	0	-	-	6500	10	70.0	5	-19.93	0.70	<20.83
127095	6863	3947	115045.56	21 147.5	14.2	5	1.4	1.4	6199	2	70.0	5	-20.03	0.80	<20.77
127096	-	3946	115045.87	211757.6	15.5	9	0.6	0.5	--	-	70.0	5	-18.76	0.49	<20.98
127111	-	3989	115452.50	253040.1	15.7	9	0.5	0.3	--	-	70.0	5	-18.61	0.72	<21.25
127112	6935	3993	1155 3.56	2531 7.7	14.8	5	1.6	0.4	4824	8	46.5	11	-19.27	0.80	<20.85
127114	6942	3997	115514.19	253256.2	14.3	5	1.6	1.3	4771	24	46.5	11	-19.15	0.79	<20.86
127117	-	3999	115522.31	252047.9	15.7	1	-	-	--	-	70.0	5	-18.60	0.97	<21.12
127118	6949	4000	115522.87	252523.5	15.2	9	1.1	0.2	4551	25	46.5	11	-18.43	1.00	<20.76
127120	6952	4005	115536.00	2524 1.9	14.1	3	1.1	0.6	4470	24	46.5	11	-19.39	1.00	<20.75
127121	-	4011	115551.31	252233.7	15.7	1	-	-	--	-	70.0	5	-18.68	0.94	<21.14
127122	6965	4015	1156 8.37	251855.4	14.2	0	-	-	4341	10	46.5	11	-19.14	0.73	<20.89
98034	-	-	12 049.94	2018 1.0	14.8	9	0.4	0.3	6561	25	70.0	5	-19.48	0.38	<21.22
98039	-	-	12 117.69	201952.3	15.7	0	-	-	--	-	70.0	5	-18.53	0.61	<21.02
128006	-	4060	12 127.50	203656.6	15.6	1	-	-	--	-	70.0	5	-18.68	0.91	<20.84
128008	7051	4066	12 135.87	203734.7	14.4	0	-	-	7386	10	70.0	5	-19.83	0.91	<20.86
128009	7052	4070	12 137.81	204116.5	14.3	0	-	-	7222	10	70.0	5	-19.93	0.76	<20.94
98045	-	4072	12 140.37	202917.1	15.6	1	-	-	--	-	70.0	5	-18.78	1.00	<20.80
128019	7077	4090	12 254.50	203511.9	15.0	1	-	-	--	-	70.0	5	-19.38	0.38	<21.22
128018	7076	4086	12 256.06	203130.7	15.1	0	-	-	--	-	70.0	5	-19.13	0.38	<21.22
128020	-	4089	12 3 4.19	2050 1.9	14.9	0	-	-	6905	9	70.0	5	-19.33	0.97	<20.84
128022	7083	4091	12 3 7.00	2050 2.3	15.2	1	-	-	--	-	70.0	5	-19.32	0.98	<20.84
160020N	-	-	125340.69	275653.6	15.5	8	0.3	0.2	4968	24	69.0	2	-18.88	0.28	<21.40
160026	-	3913	1254 6.00	2733 0.0	15.5	9	0.7	0.5	7534	6	69.0	2	-18.75	0.36	<21.30
160037	-	-	125448.00	2744 0.0	15.0	1	-	-	7341	12	69.0	2	-19.19	0.97	<20.86
160040	-	-	1255 0.00	2749 0.0	15.3	0	-	-	5523	12	69.0	2	-18.89	1.00	<20.85
160042	-	4840	1255 6.00	2753 0.0	14.8	0	-	-	5949	12	69.0	2	-19.39	0.91	<20.89
160043	8071	-	1255 6.00	2828 0.0	15.4	2	1.0	0.3	7078	12	69.0	2	-19.00	0.34	<21.22
160044	8072	4841	1255 6.90	284449.6	13.5	0	-	-	6784	10	69.0	2	-20.69	0.85	<20.82
160049	-	-	125524.00	2827 0.0	15.5	1	-	-	7359	12	69.0	2	-18.69	0.36	<21.20
160057	-	-	125548.00	2824 0.0	15.5	1	-	-	7414	12	69.0	1	-18.69	0.25	<21.37
160061	-	4851	125554.00	2825 0.0	15.2	1	-	-	7794	12	69.0	1	-18.99	0.28	<21.31
160067	-	-	125612.00	2726 0.0	15.4	8	0.3	0.3	7653	6	69.0	2	-18.79	0.53	<21.19
160068	8092	4853	125612.00	2751 0.0	14.2	0	-	-	7550	10	69.0	1	-19.99	0.44	<21.20
160070	-	4854	125624.00	2757 0.0	15.2	1	-	-	8276	12	69.0	1	-18.99	0.24	<21.46
160214	-	-	125637.05	282941.0	15.3	1	-	-	8028	12	69.0	1	-18.89	0.31	<21.26
160074	-	-	125648.73	274018.7	15.4	1	-	-	5633	12	69.0	2	-18.79	0.38	<21.33
160086	-	-	1258 8.87	275423.1	15.4	8	0.5	0.4	7476	25	69.0	1	-18.90	0.16	<21.33
160251	-	-	125811.00	282454.0	15.7	2	0.6	0.2	5536	12	69.0	1	-18.69	0.31	<21.05
160253	-	4906	125815.00	281136.0	15.2	0	-	-	7510	12	69.0	1	-18.99	0.56	<20.79
160254	-	4041	125816.49	281556.6	15.7	0	-	-	7087	12	69.0	1	-18.49	0.55	<20.80
160255	-	4042	125818.00	281412.0	15.5	1	-	-	6603	12	69.0	1	-18.69	0.58	<20.77
160256	-	4045	125824.00	282130.0	15.1	0	-	-	6865	12	69.0	1	-19.09	0.50	<20.84
160257	-	4907	125824.37	282537.8	14.6	5	1.1	0.8	5868	1	69.0	1	-19.76	0.37	<20.96
160258	-	4908	125827.00	281836.0	14.9	0	-	-	8850	12	69.0	1	-19.29	0.60	<20.76
160259	8129	4051	125829.00	281630.0	14.8	0	-	-	4926	12	69.0	1	-19.39	0.66	<20.71
160261	-	-	125834.00	2810 0.0	15.6	9	0.6	0.3	6917	12	69.0	1	-18.71	0.75	<20.66
160092	-	-	125842.00	28 5 0.0	15.7	0	-	-	5986	12	69.0	1	-18.49	0.72	<20.68
160093	-	-	125848.00	28 4 0.0	15.7	1	-	-	6522	12	69.0	1	-18.49	0.73	<20.67
160094	8133	4919	125854.00	28 4 0.0	14.9	1	-	-	7278	12	69.0	1	-19.40	0.77	<20.65
160097	-	4923	1259 6.00	28 6 0.0	14.7	1	-	-	5446	12	69.0	1	-19.49	0.90	<20.58
160100	-	-	125925.87	28 943.4	15.5	0	-	-	7626	12	69.0	1	-18.69	0.99	<20.54
160101	-	-	125924.00	2822 0.0	15.2	2	1.0	0.2	5828	12	69.0	1	-19.27	0.74	<20.66
160103	8142	4926	125930.00	2753 0.0	14.1	0	-	-	7551	10	69.0	2	-20.09	0.32	<21.02
160104	-	-	125936.00	28 3 0.0	15.4	2	0.6	0.3	7213	12	69.0	2	-18.91	0.76	<20.66
160110	-	-	13 0 0.00	2830 0.0	15.2	1	-	-	5733	12	69.0	2	-18.99	0.28	<21.09
160112	-	4106	13 012.00	2822 0.0	15.5	2	0.7	0.5	7454	12	69.0	2	-18.75	0.48	<20.85
160113	-	4929	13 018.00	2818 0.0	14.9	0	-	-	6353	12	69.0	2	-19.29	0.53	<20.81
160115	-	-	13 024.00	28 7 0.0	15.4	0	-	-	8180	12	69.0	2	-18.79	0.49	<20.85
160116	-	4111	13 030.00	2820 0.0	15.7	1	-	-	7904	12	69.0	2	-18.49	0.38	<20.95
160175	-	-	131359.62	305630.7	15.1	9	0.8	0.4	5661	25	56.6	16	-18.78	0.33	<21.22
160176	8342	5057	1314 7.12	311741.3	14.6	1	-	-	5856	12	58.6	16	-19.25	0.97	<20.78
160180	-	-	1315 0.81	311921.7	15.4	9	0.5	0.3	--	-	70.0	5	-18.91	0.76	<21.05
160181	8356	5065	131510.06	312120.9	14.3	7	1.5	0.8	5550	2	55.5	16	-19.74	0.63	<20.93
160183	-	5074	1316 5.69	314418.5	14.7	5	0.8	0.8	5604	2	56.0	16	-19.04	1.01	<20.59
160185	-	-	131611.50	3136 2.6	15.2	0	-	-	--	-	70.0	5	-19.03	0.83	<20.87
160186	-	-	131616.62	31 740.5	15.5	0	-	-	--	-	70.0	5	-18.73	0.49	<21.08
160190	-	-	131639.31	31 236.8	15.3	0	-	-	--	-	70.0	5	-18.93	0.72	<20.91
160191	-	-	131639.62	31 444.6	15.7	9	0.6	0.2	--	-	70.0	5	-18.72	0.74	<20.90
160193	-	-	131645.69	312437.5	15.6	0	-	-	--	-	70.0	5	-18.63	0.23	<21.42
160195	-	-	131727.37	31 515.8	15.7	9	0.4	0.4	--	-	70.0	5	-18.53	1.01	<20.76
160199	-	-	131747.87	304242.6	15.7	9	0.4	0.3	--	-	70.0	5	-18.58	0.17	<21.54
160201	-	-	131754.62	311459.0	15.1	0	-	-	--	-	70.0	5	-19.13	0.68	<20.94
160203	-	-	1318 5.37	305152.5	15.4	1	-	-	--	-	70.0	5	-18.83	0.47	<21.09

References to the redshift measurements in Tables II and III

1: Giovanelli and Haynes (1985).
2: Chincarini, Giovanelli, and Haynes (1983).
3: Sullivan, Bothun, Bates, and Schommer (1981).
4: Chincarini, Giovanelli, Haynes, and Fontanelli (1983).
5: Fontanelli (1984).
6: Bothun *et al.* (1985).
7: Williams and Kerr (1981).
8: Palumbo, Tanzella-Nitti, and Vettolani (1983).
9: Gregory and Thompson (1978).
10: Huchra, Davis, Latham, and Tonry (1983).
11: Huchtmeier, Richter, Bohnenstengel, and Hauschildt (1983).
12: Tifft and Gregory (1976).
13: Davis and Seaquist (1983).
14: Fisher and Tully (1981).
15: Haynes and Giovanelli (1984).
16: Dickens and Moss (1976).
17: Tifft and Tarenghi (1975).
18: Gudehus (1976).
19: Gregory (1975).
20: Fontanelli (private communication).
21: Gregory and Thompson (1977).
22: Sulentic and Arp (1982).
23: Giovanelli (private communication).
24, 25: Gavazzi (1987).
26: Kent and Gunn (1982).
27: Eder (private communication).
28: Wardle and Knapp (1986).
29: Bottinelli, Gouguenheim, and Paturel (1982).
30: Wevers, van der Kruit, and Allen (1986).
31: Kraan-Korteweg (1986).
32: Williams (1986).

galaxies already known to be radio sources at either 0.6 or 1.4 GHz with flux > 5 mJy, whose structure we wanted to determine at high resolution.

The observing-frequency bands and the calibrations were the same as in C array. A 20 min observation was obtained for each galaxy, and the data were reduced similarly to those at lower resolution. The beam sizes are in general 2–4 arcsec, except in some maps (8.2″ × 8.2″) that were produced with large cell size in order to include some strong disturbing sources at the edge of the field. The information in Table V is organized as follows: columns 1–14 list the optical information available (arranged similarly to that in Table II); columns 15–19 give the results from the A array observations (differences between optical and radio positions, rms noise,

TABLE IV. Comparison between 1.4 and 0.6 GHz measurements.

CGCG	$S_{0.6}$	$S_{1.4}$	Ref.
Galaxies detected at 610 MHz but not at 1.4 GHz			
127071	8.1	< 1.3	Pap.I
124114	7.9	< 2.8	Pap.I
127120	6.1	< 2.2	Pap.I
128008	14.3	< 1.2	Pap.I
128019	6.6	< 2.9	Pap.I
128018	4.0	< 2.9	Pap.I
160020	12.2	< 4.4	JPV
160086	5.8	< 3.7	JPV
160183	10.0	< 1.0	Pap.I, wrong ID
Galaxies detected at 1.4 GHz but not at 610 MHz			
97089	< 6.4	1.5	A1367
97092	<25.2	2.9	"
97114	<30.0	4.0	"
97120	<30.3	4.7	"
98041	<80.0	2.5	Pap.I
98042	<80.0	3.4	Pap.I
160046	< 6.2	1.9	Coma
160106	< 9.3	1.6	"
160108	< 9.5	7.6	"
128023	<100.0	9.4	Pap.I (see Fig.1)
Good associations that were dubious 0.6 GHz.			
127088	6.3	2.6	
127092	68.3	52.4	
128024	100.4	80.6	
160187	16.1	8.0	

1.4 GHz core flux and beam size); columns 20 and 21 give the available 1.4 GHz sky flux and largest angular size obtained from low-resolution observations (C array).

The contour maps of the extended sources are presented in Fig. 3, except for 98040 and 160039, which are given in Fig. 1.

127040 (Fig. 3(a)): the source was detected in C array at the north edge of the field A1367NW (Paper II). It consists of three components. Only the two southern ones are tentatively identified with the galaxy.

98040 (Fig. 1(c)): in A array we detect the beginning of a symmetrical jet (10 arcsec each side of the nucleus, 9.3 mJy) and a second enhancement of the jet 30 arcsec to the east (5.0 mJy).

128034 (Fig. 3(b)): A array reveals a bright (48 mJy) core and the beginning of an asymmetrical jet pointing to SE. The component further to the SE (16.9 mJy), in spite of its morphology, which resembles that of a triple radio galaxy, has no optical counterpart on the Palomar Sky Survey and it is tentatively associated with 128034 (see C array map in Paper II).

160008 (Fig. 3(c)): we reveal the beginning of a symmetrical jet in this wide-angle-tail radio galaxy studied by Giovannini (1986).

V. DISCUSSION AND CONCLUSIONS

a) The Spectral-Index Distribution

The spectral indexes of 52 galaxies observed in the present survey and at 0.6 GHz and detected at least at one frequency are given in Table VI arranged as follows: for every galaxy, the type and aggregation parameter are given followed by the sky flux at 0.6 GHz with error and by the sky flux at 1.4 GHz with error. The last two columns give the spectral index with error. The quoted flux errors are a combination of the errors in the map fluxes, which are taken as 10% of the flux densities, and the errors in the attenuation factor, which are estimated as $10R$ %, where R is the distance in degrees from the field center.

Among these 52 galaxies, a subsample of 16 objects with reliable estimates of α ($\sigma_\alpha < 0.25$) was obtained by considering only those sources with a signal-to-noise ratio > 8 and with primary-beam attenuation factor > 0.40. For these we derive $\langle\alpha\rangle = 0.78 \pm 0.09$, consistent with $\langle\alpha\rangle = 0.8$ as-

TABLE V. Galaxies observed in A array.

Optical														A array					C array		
(1)	(2)	(3)	(4)	(5)	(6)	(7)	(8)	(9)	(10)	(11)	(12)	(13)	(14)	(15)	(16)	(17)	(18)	(19)	(20)	(21)	
CGCG	UGC	NGC	R.A.	Dec.	m_p	T	a	b	Vel	R	Dist	A	M	$\alpha_0-\alpha_r$	S_0-S_r	rms	S_{sky}	FWHM	S_{sky}	LAS	Notes
March 9, 1986																					
128008	7051	4066	12 135.87	203734.7	14.4	0	-	-	7386	10	70.0	5	-19.83	-	-	0.15	< 0.60	3.5X3.5	< 1.08	71	
128023	7087	4092	12 317.00	204518.7	14.4	3	1.1	1.1	6719	2	70.0	5	-19.83	-	-	0.36	< 1.44	3.5X3.5	9.38	-	
128034	7115	-	12 532.62	253057.1	14.4	0	-	-	6767	10	70.0	5	-19.83	-1.86	1.69	0.18	70.90	3.5X3.5	242.21	360	1
158045	7211	4175	12 959.12	292647.6	14.2	2	2.1	0.4	3956	24	39.0	13	-19.04	0.11	0.50	0.14	16.90	4.7X4.7	26.83	8	
158077	7386	4278	121736.44	293329.7	11.2	0	-	-	630	10	9.8	18	-18.76	4.46	1.69	-	330.00	3.5X3.5	476.19	25	2
159072	7938	4676	124344.25	31 017.8	14.1	5	2.2	0.4	6613	2	66.1	7	-20.91	3.21	-0.50	0.12	12.00	3.5X3.5	15.09	-	8
101006	8248	-	13 8 0.25	184214.9	14.8	5	1.1	0.4	3710	23	38.4	15	-18.66	-0.83	1.13	0.12	1.30	4.7X4.7	13.91	12	
130015	-	856	13 815.37	2048 8.0	15.2	2	0.8	0.3	4049	24	38.4	15	-17.89	-	-	0.15	< 0.60	4.7X4.7	9.00	15	
March 10, 1986																					
157005	-	3781	113627.00	263816.6	14.8	2	0.5	0.4	6798	24	70.0	6	-19.46	3.13	-2.81	0.23	26.70	3.5X3.5	36.39	-	
157018	-	3826	113956.44	264557.8	14.4	0	-	-	9051	10	90.5	19	-20.38	1.23	-0.63	0.27	28.70	3.5X3.5	24.49	-	
97073	-	-	114020.75	201441.8	15.6	8	0.5	0.5	7275	24	65.0	3	-18.46	-	-	0.26	< 1.04	8.2X8.2	17.04	58	
97079	-	-	114037.50	201656.8	15.7	8	0.5	0.4	7000	24	65.0	3	-18.47	0.00	-0.75	0.28	1.20	8.2X8.2	3.87	25	
127040	-	-	114051.00	203634.3	15.3	1	-	-	--	-	65.0	3	-18.96	0.00	1.50	0.18	31.40	2.3X2.3	45.79	7	1
97087	6697	-	114113.19	201449.1	14.3	8	1.7	0.3	6723	24	65.0	3	-20.56	2.64	0.00	0.29	3.70	3.5X3.5	58.06	120	
127063	6800	3910	114724.19	213641.4	14.4	0	-	-	7840	10	70.0	5	-19.83	-	-	0.25	< 1.00	2.3X2.3	< 1.24	-	5
127092	-	-	115036.31	205612.1	15.3	0	-	-	--	-	70.0	5	-18.93	0.00	-1.00	0.19	37.00	2.3X2.3	52.39	-	
98040	7044	4061	12 127.87	203038.0	14.4	0	-	-	7336	10	70.0	5	-19.83	-1.87	-0.56	0.18	14.30	4.7X4.7	316.81	150	1,9
98042	7050	4065	12 132.81	203047.7	14.0	0	-	-	6374	10	70.0	5	-20.23	1.58	-0.19	0.18	3.00	4.7X4.7	3.40	-	1,2
160008	8028	4789	125153.35	272020.2	13.3	1	-	-	8224	12	69.0	2	-20.94	2.83	1.13	0.17	22.80	2.3X2.3	90.28	480	1,4,6
160028	8065	4827	125418.12	272656.9	14.1	1	-	-	7650	10	69.0	2	-20.12	0.72	0.81	0.21	8.70	8.2X8.2	58.42	210	6
160039	8070	4839	125459.00	2746 6.6	13.6	0	-	-	7446	10	69.0	2	-20.59	-1.27	3.81	0.13	44.00	2.3X2.3	74.54	34	1,4,7
160055	8082	4848	125540.69	283044.4	14.2	8	1.5	0.3	7049	1	69.0	1	-20.74	-0.22	-0.63	0.26	5.60	3.5X3.5	23.21	-	
160058	-	-	125544.81	285841.0	15.5	6	1.0	0.3	7609	1	69.0	2	-19.28	-	-	0.15	< 0.60	3.5X3.5	1.54	-	
160056	8086	4849	125547.25	263959.9	14.5	1	-	-	5885	10	69.0	2	-19.77	2.07	-0.13	0.10	8.34	3.5X3.5	23.21	15	
160213	-	4858	125637.31	2823 6.2	15.5	8	0.4	0.3	9386	1	69.0	1	-18.83	0.77	-1.31	0.21	2.20	8.2X8.2	6.77	-	
160252	-	4040	125813.62	281934.0	15.1	8	0.6	0.2	7850	25	69.0	1	-19.60	3.41	-1.19	0.13	5.80	8.2X8.2	23.97	-	
160260	8128	4911	125831.00	28 336.0	13.7	5	1.0	0.7	7970	1	69.0	1	-20.68	-	-	0.09	< 0.40	8.2X8.2	18.12	-	
160098	-	-	1259 0.87	285712.0	15.3	8	0.6	0.5	8762	1	69.0	2	-18.98	-	-	0.23	< 0.92	3.5X3.5	7.25	-	3
160124	8167	4944	13 125.87	282713.2	13.3	1	-	-	7111	25	69.0	2	-21.06	-	-	0.10	< 0.40	3.5X3.5	-	-	

Notes to TABLE V

1 See contour map
2 Positions and flux derived from contour map
3 Flux derived from the 610 MHz observation with α =0.8
4 LAS is the separation between the double component
5 Galaxy misidentified at 610 MHz
6 See Giovannini, 1987
7 See Parma et al., 1986
8 Values refer to N component of double system. See high sensitivity map in Hummel, et al, 1987
9 Compare with Burns, et al, 1987

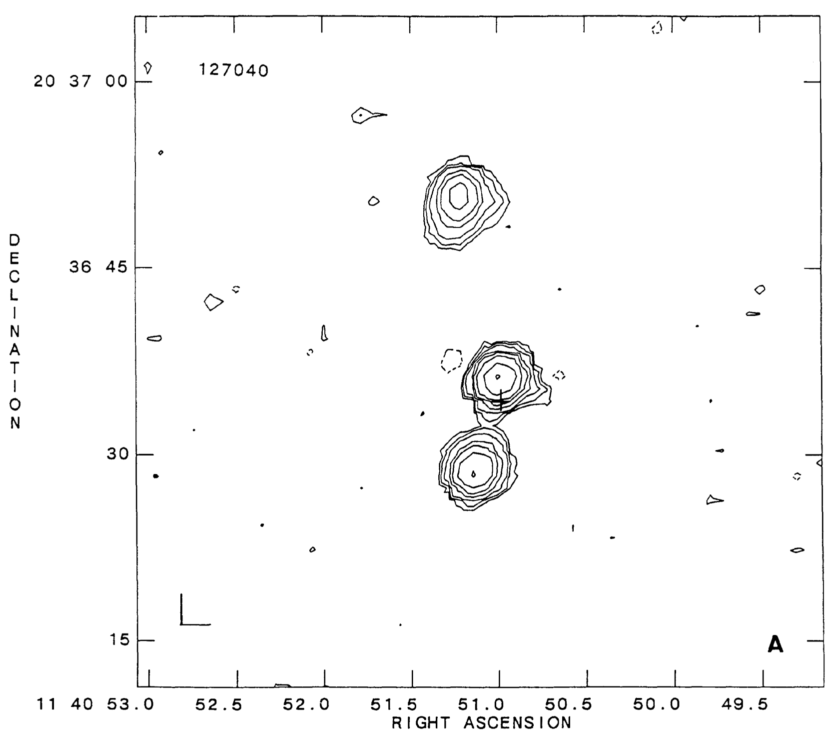

FIG. 3. Contour maps of the interesting galaxies detected in A array. The cross marks the position of the parent galaxy. The L shaped symbol in the lower left-hand corner indicates the FWHM of the beam. (a): 127040 (levels: 0.4, 0.7, 1.2, 2.4, 3.6, 6.0, 12.0, and 24.0 mJy/beam). (b): 128034 (levels: 0.7, 1.2, 2.0, 4.0, 6.0, 10.0, 20.0, and 40.0 mJy/beam). (c): 160008 (levels: 0.9, 1.35, 2.4, 3.0, and 4.5 mJy/beam).

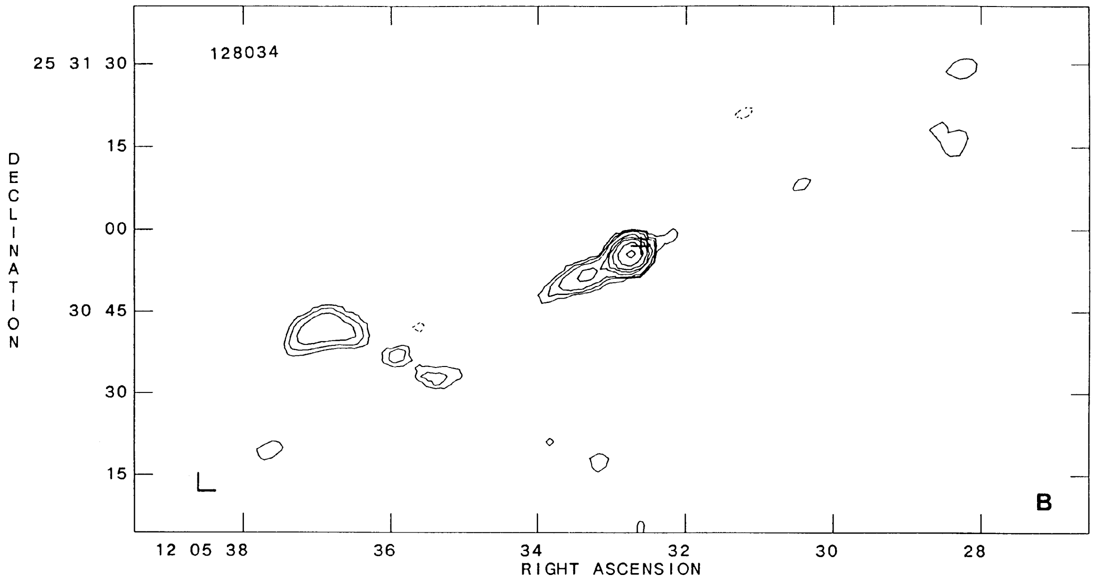

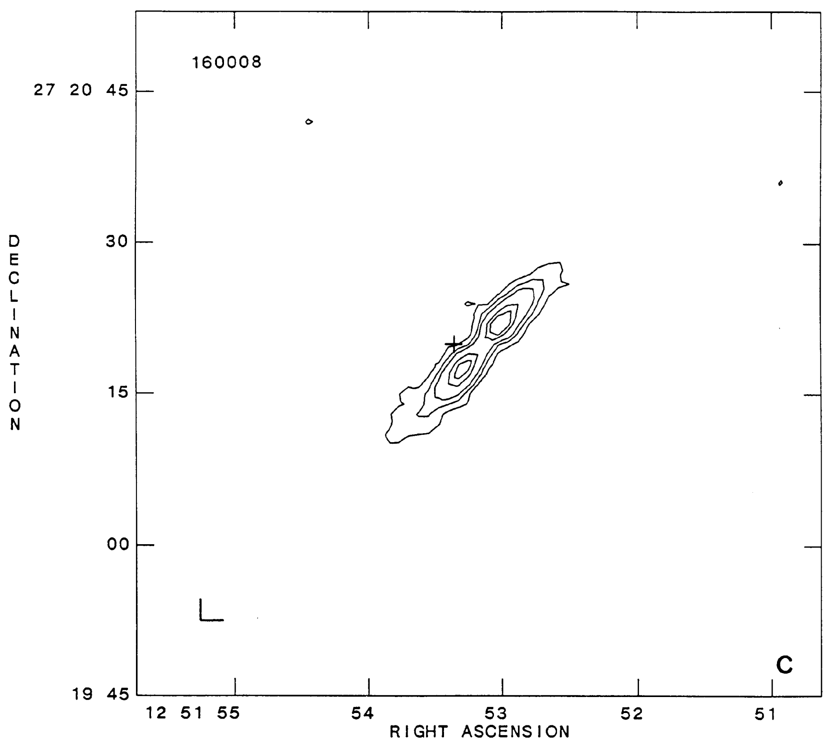

FIG. 3. (continued)

TABLE VI. 0.6 to 1.4 GHz spectral index.

Name	T	Agg	$S_{0.6}$	$\sigma_{0.6}$	$S_{1.4}$	$\sigma_{1.4}$	α	σ_α
97068	6	3	28.60	4.40	8.14	0.85	1.41	0.21
97073	8	3	30.00	-	17.04	1.71	0.63	-
97079	8	3	32.40	-	3.87	0.40	2.38	-
127040	1	3	< 34.56	-	51.93	5.50	<-0.46	-
97087	8	3	128.10	13.51	58.06	5.86	0.89	0.16
97089	0	3	< 6.40	-	1.53	0.21	< 1.60	-
97092	9	3	< 25.20	-	2.88	0.35	< 2.43	-
97091	6	3	11.20	2.19	2.29	0.27	1.78	0.26
97095	0	3	43.60	4.76	15.54	1.59	1.16	0.17
97114	8	3	< 30.00	-	4.03	1.11	< 2.25	-
97120	3	3	< 30.32	-	4.69	1.16	< 2.09	-
97127	0	3	10790.00	1093.54	5333.04	540.09	0.79	0.16
127071	8	5	8.10	1.94	< 1.28	-	> 2.07	-
127092	0	5	68.30	7.61	52.39	5.33	0.30	0.17
127110	6	11	58.90	6.16	33.69	3.51	0.63	0.17
127114	6	11	7.90	1.56	< 2.79	-	> 1.17	-
127120	5	11	6.10	1.44	< 2.19	-	> 1.15	-
127123	7	11	36.50	4.00	5.06	1.13	2.21	0.28
98040	1	5	498.00	49.83	316.81	31.72	0.51	0.16
98042	0	5	< 80.00	-	3.40	0.44	< 3.54	-
128008	0	5	14.30	1.66	< 1.23	-	> 2.75	-
98041	8	5	< 80.00	-	2.46	0.38	< 3.90	-
128013	1	5	6.70	1.05	2.02	0.36	1.34	0.27
98046	3	5	8.50	1.17	2.12	0.37	1.55	0.25
128019	1	5	6.60	1.16	< 2.94	-	> 0.91	-
128018	0	5	4.00	1.01	< 2.93	-	> 0.35	-
128023	3	5	< 100.00	-	9.38	0.98	< 2.65	-
128024	0	5	100.40	11.28	80.65	8.07	0.25	0.17
128025	0	5	6.60	1.46	3.35	0.45	0.76	0.29
160008	1	2	82.50	33.04	90.28	9.41	-0.10	0.46
160020	8	2	12.20	3.35	< 4.37	-	> 1.15	-
160028	1	2	88.50	12.93	58.42	6.06	0.47	0.20
160039	0	2	182.00	20.96	74.54	7.46	1.00	0.17
160041	2	2	< 124.08	-	1.66	0.23	< 4.83	-
160046	0	2	< 6.16	-	1.87	0.36	< 1.33	-
160055	8	1	44.50	5.09	23.21	2.43	0.73	0.17
160058	6	2	12.50	4.26	1.54	0.47	2.34	0.51
160064	8	2	8.50	3.06	1.95	0.53	1.65	0.50
160213	8	1	17.00	2.33	6.77	0.75	1.03	0.20
160224	0	1	< 4.12	-	2.74	0.35	< 0.46	-
160225	0	1	1173.00	117.66	354.53	35.75	1.34	0.16
160231	0	1	400.00	40.38	196.72	19.75	0.79	0.16
160086	8	1	5.80	2.10	< 3.76	-	> 0.49	-
160252	8	1	33.70	4.04	23.97	2.44	0.38	0.18
160260	5	1	34.60	4.28	18.03	1.86	0.73	0.18
160095	5	1	7.40	2.42	6.47	0.67	0.15	0.38
160105	1	1	9.60	3.05	7.08	0.73	0.34	0.37
160106	8	2	< 9.32	-	1.58	0.43	< 1.99	-
160108	8	2	< 9.52	-	7.65	0.90	< 0.24	-
160173	7	16	15.30	2.83	3.99	0.57	1.50	0.26
160187	1	5	16.10	3.47	8.03	0.85	0.78	0.27
160200	1	5	8.80	1.43	2.28	0.37	1.51	0.26

sumed throughout Paper III. Due to the limited statistics, we do not attempt to estimate systematic differences in the spectral properties of galaxies in various density environments.

b) The Structures

A and C array measurements at 1.4 GHz are available for 26 galaxies in our sample. For these objects, we derive the percentage of flux in the core with respect to total flux as a function of morphological type. It appears that the contribution of the central source to the total flux decreases from elliptical (58%) to S0–S0a (36%), Sb–Sbc (27%), and irregular galaxies (19%), in agreement with the results of Hummel (1981) and Condon (1983). Only two S/Irr galaxies, i.e., 160252 and 160260, both unresolved or barely resolved in C array and with either a weak or an undetected core component, have a useful lower limit to the size of their extended component. In both cases it corresponds to the size of the optical disk.

c) The Radio Luminosity Function

None of the conclusions of the statistical analysis carried out in Paper III on the radio-continuum properties of galaxies in the Coma supercluster are significantly influenced by the data presented in this paper. In particular, the 1.4 GHz radio luminosity function derived in Paper III for 728 galaxies in the Coma/A1367 supercluster region was based on 284 objects observed at 0.6 GHz and on 444 objects measured at 1.4 GHz, with the former converted to 1.4 GHz using $\langle\alpha\rangle = 0.8$. Using the new 148 measurements presented in this paper (with the remaining 136 observed at 0.6 GHz still converted to 1.4 GHz using $\langle\alpha\rangle = 0.8$), we obtain a qualitative agreement with the radio luminosity functions derived in Paper III. As an example, the distribution of the radio to optical luminosity function for spiral galaxies in and outside rich clusters is shown in Fig. 4. We confirm that spirals in clusters have radio/optical luminosities ≈ 4 times higher than those in regions of lower galaxy density. Since their optical luminosity distribution does not differ appreciably in the two samples, we confirm that spiral and irregular galaxies in the two studied clusters have average radio luminosities ≈ 4 times higher than similar galaxies in the sparse supercluster population. This value results from a combination of a factor of 10 difference found among late-type spirals and a marginal difference in the early-type sample, as shown in Fig. 6 of Paper III.

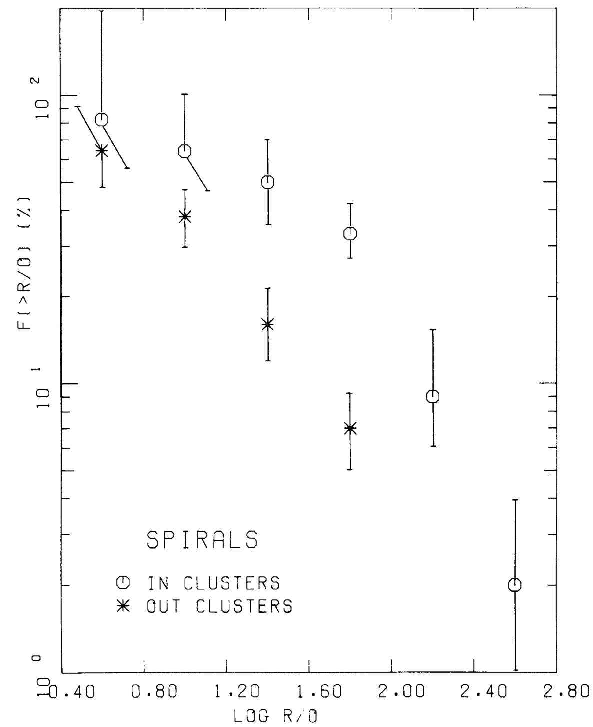

FIG. 4. Integral distribution of the ratio of radio to optical luminosity for spiral + irregular galaxies inside (O) and outside (*) rich clusters in the Coma supercluster.

REFERENCES

Bothun, G. D., Aaronson, M., Schommer, R. A., Mould, J., Huchra, J., and Sullivan III, W. T. (1985). Astrophys. J. Suppl. **57**, 423.

Bottinelli, L., Gouguenheim, L., and Paturel, G. (1982). Astron. Astrophys. Suppl. **47**, 171.

Burns, J., Hanisch, R., White, R., Nelson, E., Morrisette, K., and Moody, J. W. (1987). Astron. J. **94**, 587.

Chincarini, G. L., Giovanelli, R., and Haynes, M. P. (1983). Astrophys. J. **269**, 13.

Chincarini, G. L., Giovanelli, R., Haynes, M. P., and Fontanelli, P. (1983). Astrophys. J. **267**, 511.

Condon, J. J. (1983). Astrophys. J. Suppl. **53**, 459.

Davis, L. E., and Seaquist, E. R. (1983). Astrophys. J. Suppl. **53**, 269.

Dickens, R. J., and Moss, C. (1976). Mon. Not. R. Astron. Soc. **174**, 47.

Fisher, J. R., and Tully, R. B. (1981). Astrophys. J. Suppl. **47**, 139.

Fontanelli, P. (1984). Astron. Astrophys. **138**, 85.

Gavazzi, G. (1979). Astron. Astrophys. **72**, 1.

Gavazzi, G. (1987). Astrophys. J. **320**, 96.

Gavazzi, G., and Jaffe, W. (1986). Astrophys. J. **310**, 53 (Paper III).

Gavazzi, G., Perola, C., and Jaffe, W. (1981). Astron. Astrophys. **35**, 103.

Giovanelli, R., and Haynes, M. P. (1985). Astrophys. J. **292**, 404.

Giovannini, G. (1986). In *Proceedings of the Conference on Radio Continuum Processes in Clusters of Galaxies*, edited by C. O'Dea and J. Uson (NRAO, Green Bank), p. 215.

Gregory, S. A. (1975). Astrophys. J. **199**, 1.

Gregory, S. A., and Thompson, L. A. (1977). Astrophys. J. **213**, 345.

Gregory, S. A., and Thompson, L. A. (1978). Astrophys. J. **222**, 784.

Gudehus, D. H. (1976). Astrophys. J. **208**, 267.

Haynes, M. P., and Giovanelli, R. (1984). Astron. J. **89**, 758.

Huchra, J., Davis, M., Latham, D., and Tonry, J. (1983). Astrophys. J. Suppl. **52**, 89.

Huchtmeier, W. K., Richter, O. G., Bohnenstengel, H. D., and Huschildt, M. (1983). *A General Catalogue of HI Observations of External Galaxies*, ESO Preprint No. 205 (ESO, Garching).

Hummel, E. (1981). Astron. Astrophys. **93**, 93.

Hummel, E., van der Hulst, J., Keel, W., and Kennicutt, R. (1987). Astron. Astrophys. Suppl. **70**, 517.

Jaffe, W., and Gavazzi, G. (1986). Astron. J. **91**, 204 (Paper II).

Jaffe, W., Gavazzi, G., and Valentijn, E. (1986). Astron. J. **91**, 199 (Paper I).

Jaffe, W., Perola, G. C., and Valentijn, E. (1976). Astron. Astrophys. **49**, 179 (JPV).

Kent, S. M., and Gunn, J. E. (1982). Astron. J. **87**, 945.

Kraan-Korteweg, R. (1986). Astron. Astrophys. Suppl. **66**, 255.

Nilson, P. (1973). *Uppsala General Catalogue of Galaxies*, Uppsala Astron. Obs. Ann. **6** (UGC).

Palumbo, G., Tanzella-Nitti, G., and Vettolani, P. G. (1983). *Catalogue of Radial Velocities of Galaxies* (Gordon and Breach, New York).

Parma, P., de Ruiter, H. R., Fanti, C., and Fanti, R. (1986). Astron. Astrophys. Suppl. **64**, 135.

Sulentic, J. W., and Arp, H. (1982). Astron. J. **88**, 489.

Sullivan, W. T., Bothun, G. D., Bates, B., and Schommer, R. A. (1981). Astron. J. **86**, 919.

Thompson, A. R., Clark, B. G., Wade, C. M., and Napier, P. J. (1980). Astrophys. J. Suppl. **44**, 151.

Tifft, W. G., and Gregory, S. A. (1976). Astrophys. J. **205**, 696.

Tifft, W. G., and Tarenghi, M. (1975). Astrophys. J. Lett. **198**, L7.

Wardle, M., and Knapp, G. R. (1986). Astron. J. **91**, 23.

Wevers, B., van der Kruit, P., and Allen, R. (1986). Astron. Astrophys. Suppl. **66**, 505.

Williams, B. A. (1986). Astrophys. J. **311**, 25.

Williams, B. A., and Kerr, F. J. (1981). Astron. J. **86**, 953.

Zwicky, F., and Herzog, E. (1963). *Catalogue of Galaxies and Clusters of Galaxies* (California Institute of Technology, Pasadena) (CGCG).

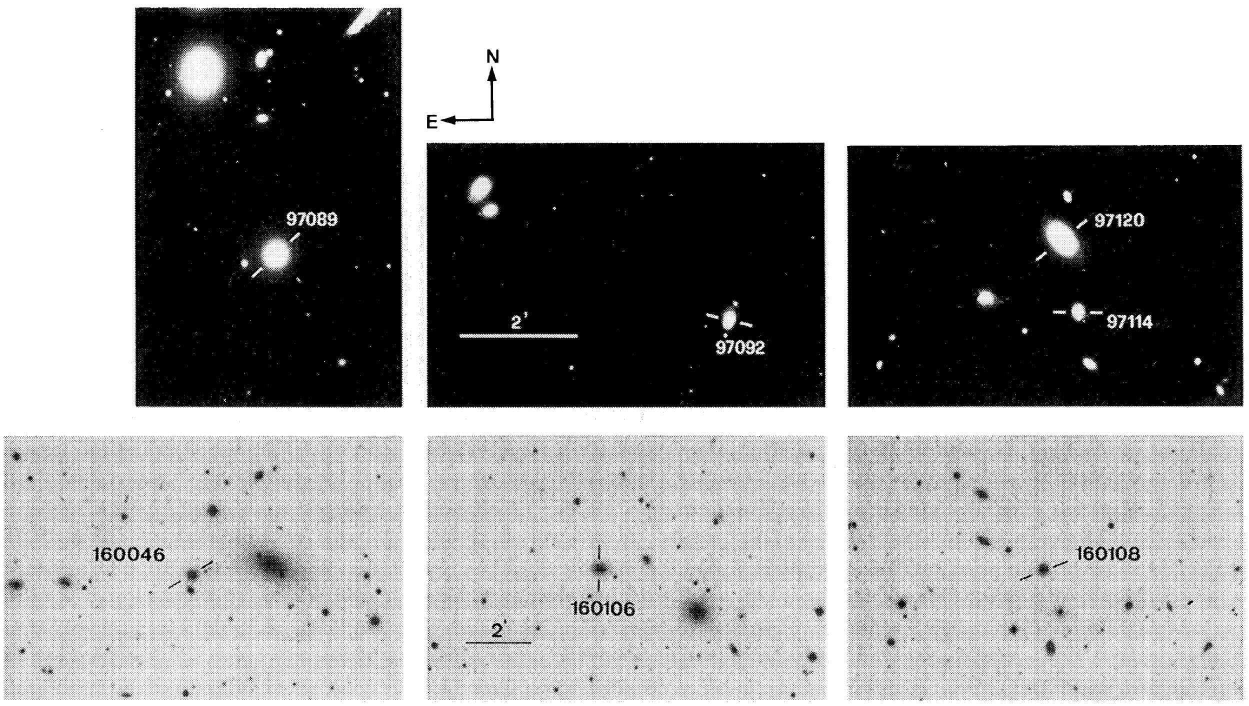

FIG. 2. Finding chart of the newly identified galaxies in A1367 (upper: enlargement of a 4 m plate kindly made available by A. Oemler) and in the Coma cluster (lower: enlargement of the Palomar Sky Survey Atlas. ©1960 National Geographic Society—Palomar Sky Survey. Reproduced by permission of the California Institute of Technology.

del Castillo *et al.* (see page 1341)